Cerebral Cortex April 2009;19:951–962
doi:10.1093/cercor/bhn130
Advance Access publication September 18, 2008

L2/3 Interneuron Groups Defined by Multiparameter Analysis of Axonal Projection, Dendritic Geometry, and Electrical Excitability

Moritz Helmstaedter[1], Bert Sakmann[1] and Dirk Feldmeyer[2,3]

[1]Department of Cell Physiology, Max-Planck Institute for Medical Research, Jahnstrasse 29, D-69120 Heidelberg, Germany, [2]Forschungszentrum Jülich, Institut für Neurowissenschaften und Biophysik, INB-3 Medizin, Leo-Brandt-Strasse, D-52425 Jülich, Germany and [3]Department of Psychiatry and Psychotherapy, University Hospital Aachen, RWTH Aachen University, Pauwelsstrasse 30, D-52074 Aachen

For a detailed description of the circuitry of cortical columns at the level of single neurons, it is essential to define the identities of the cell types that constitute these columns. For interneurons (INs), we described 4 "types of axonal projection patterns" in layer 2/3 (L2/3) with reference to the outlines of a cortical column (Helmstaedter et al. 2008a). In addition we quantified the dendritic geometry and electrical excitability of 3 types of the L2/3 INs: "local," "lateral," and "translaminar" inhibitors (Helmstaedter et al. 2008b). Here, we used an iterated cluster analysis (iCA) that combines axonal projection patterns with dendritic geometry and electrical excitability parameters to identify "groups" of INs, from a sample of 39 cells. The iCA defined 9 groups of INs. We propose a hierarchical scheme for identifying L2/3 INs. First, L2/3 INs can be classified as 4 types of axonal projections. Second, L2/3 INs can be subclassified as 9 groups with a high within-group similarity of dendritic, axonal, and electrical parameters. This scheme of identifying L2/3 INs may help to quantitatively describe inhibitory effects on sensory stimulus representations in L2/3 of cortical columns.

Keywords: axons, barrel cortex, cluster analysis, dendrites, electrical excitability, GABAergic interneuron, lateral inhibition, layer 2/3

Introduction

Layer 2/3 (L2/3) of a single column in rat barrel cortex is estimated to comprise 3000–4000 neurons (Beaulieu 1993; for an estimate referring to the D2 barrel column, see Lübke et al. 2003). Approximately, 300–800 (10–20%, Beaulieu 1993) are assumed to be nonpyramidal neurons. Instead of separately describing each of the 800 L2/3 interneurons (INs) in a column, a reduction to "groups" of INs that share common functional and anatomical properties is expected to be sufficient for a description of their function in a column. The number of such groups of INs is not known a priori. INs that belong to the same *group* are defined to be significantly more similar with reference to axonal projection patterns, dendritic geometry, and electrical excitability than are INs that belong to different groups. In a random sample of 39 INs in L2/3 in barrel columns, an analysis of similarity between the INs in the sample is expected to yield a lower estimate for the number of groups and to allow a definition of these "IN groups." For quantitatively defining IN groups, it is crucial to use a sample of INs that has not been preselected using morphological, electrical, or immunohistochemical parameters (e.g., Gibson et al. 1999; Cauli et al. 2000; Dumitriu et al. 2007) and to avoid qualitative parameter descriptions (e.g., Gupta et al. 2000; Krimer et al. 2005). Here, we used 11 parameters for an iterated cluster analysis (iCA) to reveal similarity groups in a high-dimensional parameter space with relatively small number of cells (n = 39; the analysis of axonal, dendritic, and electrical parameters of this sample of INs was reported in 2 preceding studies [Helmstaedter et al. 2008a, 2008b]). The iCA allowed to define 9 groups of INs in L2/3.

Methods

Preparation and Solutions

All procedures were as described in the accompanying manuscript (Helmstaedter et al. 2008b). Briefly, slices of P20–29 Wistar rat somatosensory cortex were cut at 350 μm thickness in a thalamocortical plane (Agmon and Connors 1991) at an angle of 50° to the interhemispheric sulcus. Slices were incubated at room temperature (22–24 °C) in an extracellular solution containing 4 mM $MgCl_2$/1 mM $CaCl_2$. During the experiments, slices were continuously superfused with an extracellular solution containing (in mM): 125 NaCl, 2.5 KCl, 25 glucose, 25 $NaHCO_3$, 1.25 NaH_2PO_4, 2 $CaCl_2$, and 1 $MgCl_2$ (bubbled with 95% O_2 and 5% CO_2). The pipette (intracellular) solution contained (in mM): 105 K-gluconate, 30 KCl, 10 4-(2-hydroxyethyl)-1-piperazineethanesulfonic acid, 10 phosphocreatine, 4 ATPMg, and 0.3 GTP (adjusted to pH 7.3 with KOH); the osmolarity of the solution was 300 mOsm. Biocytin (Sigma, Munich, Germany) at a concentration of 3–6 mg/ml was added to the pipette solution, and cells were filled during 1–2 h of recording. All experimental procedures were performed according to the animal welfare guidelines of the Max-Planck Society.

Identification of Barrels and Neurons

All procedures were as described in the accompanying manuscript (Helmstaedter et al. 2008b). Briefly, slices were placed in the recording chamber barrels and were identified as evenly spaced, light "hollows" separated by narrow dark stripes (Agmon and Connors 1991; Feldmeyer et al. 1999) under bright-field illumination, and photographed using a frame grabber for later analysis. INs were searched in L2/3 above barrels of 250 μm ± 70 μm width (n = 64) using a water immersion objective 40×/0.80 NA and infrared differential interference contrast microscopy (Dodt and Zieglgansberger 1990; Stuart et al. 1993). Somata of neurons in L2/3 were selected for recording if a single apical dendrite was not clearly visible. This was the sole criterion for the a priori selection of INs. This selection criterion regularly resulted in recordings of pyramidal neurons, such that the remaining bias could be assumed to be small. Recordings were completed irrespective of the electrical properties of the neuron. After recording, the pipettes were positioned above the slice at the position of the recorded cells, and the barrel pattern was again photographed using bright-field illumination.

Histological Procedures

All procedures were as described in the accompanying manuscript (Helmstaedter et al. 2008b). After recording, slices were fixed at 4 °C for at least 24 h in 100 mM PB, pH 7.4, containing either 4% paraformaldehyde or 1% paraformaldehyde and 2.5% glutaraldehyde. Slices were incubated in 0.1% Triton X-100 solution containing avidin-biotinylated

horseradish peroxidase (ABC-Elite; Camon, Wiesbaden, Germany); subsequently, they were reacted using 3,3′-diaminobenzidine as a chromogen under visual control until the dendritic and axonal arborizations were clearly visible. To enhance staining contrast, slices were occasionally postfixed in 0.5% OsO_4 (30–45 min). Slices were then mounted on slides, embedded in Moviol (Clariant, Sulzbach, Germany), and enclosed with a coverslip of 0.04–0.06 mm thickness (Menzel Thermo Fisher Scientific, Braunschweig, Germany) to minimize squeezing of the slice.

Reconstruction of Neuronal Morphologies

Subsequently, neurons were reconstructed with the aid of Neurolucida software (MicroBrightField, Colchester, VT) using an Olympus Optical (Hamburg, Germany) BX50 microscope at a final magnification of ×1000 using a 100×, 1.25 NA objective. The reconstructions provided the basis for the quantitative morphological analysis (see below). The pial surface of the slice was also reconstructed. The reconstruction was rotated in the plane of the slice such that the pial surface above the reconstructed neuron was horizontally aligned. Thus, the *x*-axis of the reconstruction was parallel to the pia in the plane of the slice and the *y*-axis perpendicular to the pia in the plane of the slice.

Morphometric and Electrical Excitability Parameters

"Axonal laterality" and "verticality" with reference to the borders and layers of a cortical column were calculated as described previously (Helmstaedter et al. 2008a). Briefly, the "laterality" of the axonal projection was defined by the ratio of the total axonal path length of a neuron that extended outside of the home column, n_{lat}, and the total horizontal extent of the axon dx_{90lat}. The total horizontal extent of the axon (dx_{90lat}) was calculated as the horizontal extent of the 90% contour of the axon in units of the width of the home column (for details, cf. Helmstaedter et al. 2008a).

The calculation of dendritic polarity, dendritic path length, and electrical parameters was as in Helmstaedter et al. 2008b.

Sample Selection

Two previous studies reported axonal, dendritic, and electrical properties of a sample of 64 L2/3 INs (Helmstaedter et al. 2008a, 2008b). Electrical properties were analyzed for all these 64 INs (Helmstaedter et al. 2008b) with the exception of action potential (AP) threshold (n = 56). The dendritic arbor of 7 of 64 INs displayed insufficient staining for quantitative analysis; thus, dendritic and electrical properties were analyzed simultaneously for 57 INs (including AP threshold potential: n = 49 neurons). The axonal arbor of 51 INs met the criteria for completeness of axonal reconstruction (≥4 mm axonal path length, Helmstaedter et al. 2008a); thus, axonal and electrical properties were analyzed simultaneously for 51 INs. Axonal, dendritic, and all electrical properties could be analyzed simultaneously for 39 INs. These 39 INs therefore formed the basis for the cluster analysis (CA) presented in this study. The 4 L2/3 pyramidal neurons used as control group were the same as used in the previous study (Helmstaedter et al. 2008b).

Cluster Analyses

For the CA, 11 parameters were used (Table 1). Four L2/3 pyramidal cells were also included as control group (the pyramidal neurons were recorded under identical experimental conditions). The data matrix of size 43 × 11 (39 INs + 4 pyramidal neurons × 11 parameters) was normalized for each parameter as min–max normalization followed by log-normalization $x_i = \log(1 + x_i)$. The log-normalization did not affect the clustering results as tested a posteriori. For each parameter, a weight was randomly drawn from a uniform distribution (cf. Table 1). The sum of the weights of dendritic parameters, the sum of the weights of axonal parameters, and the sum of the weights of electrical parameters were all equal (Table 1). Equally distributed noise of half-width 0.05 was added to each entry in the data matrix. A total of 0–6 neurons were randomly excluded from the data matrix (random generator, on average in 25% of the analyses ≥1 cells were excluded). The CA was performed using centroid linkage with Euclidean distances. A maximum cluster size was implemented as a linkage distance increase that depended on the cluster size of each of the clusters to be linked in each step (the relative linkage distance increase $\Delta d_L(n_1, n_2)$ in dependence of the 2 cluster sizes n_1, n_2 to be linked was as follows:

$$\Delta d_L(n_1, n_2) = 10 \times \left[\left(1 - e^{-1/2 \times (n_1 - 1)}\right)^8 + \left(1 - e^{-1/2 \times (n_2 - 1)}\right)^8\right].$$

The CA was made until all neurons were linked. Then, the linkage step at which the 4 pyramidal cells were linked in one group was determined. This linkage distance was used as cutoff distance. If clusters of size >6 were generated before all pyramidal cells were linked, the step at which the last cluster of size <7 was generated was used as cutoff. Then, all pairs of neurons that were linked into one cluster up to the cutoff were recorded (Fig. 1*D*) and yielded an increase in the linkage count histogram as shown in Figure 2*A*. This CA (single CA) was iterated 1200 times. The counts for the 941 pairs of neurons were sorted, and groups were relinked stepwise starting from the most frequently associated pairs backwards, using the single-linkage method. The maximal cluster size was set to 7, 6, and 5 for "local," "lateral," and "translaminar inhibitors," respectively (adapted to the sample size for each "type").

As control, the data matrix was randomly shuffled for each parameter (shuffling within columns of the data matrix). Then, the CA was performed 900 times as described. The resulting linkage count histogram was analyzed (cf. Fig. 2*B*), and a Gaussian function was fitted to the histogram. The mean + 3 standard deviations (SDs) was defined as noise level cutoff (scaled to the total count of 1200), that is, 200 counts were used as cutoff. All iterated CAs were made using custom-made software written in IGOR (Wavemetrics, Lake Oswego,

Table 1
Summary of parameter weights used in the iCA

	Parameters	Average weight ± weight variation	Parameter group normalization	Effective average weight
Axonal projection	Laterality	0.75 ± 0.25	Σ=1	0.75
	Verticality	1 −laterality		0.25
Intrinsic electrical excitability	AHP adaptation	0.5 ± 0.5		0.246
	Somatic input resistance	0.5 ± 0.5		0.246
	AP half-width	0.5 ± 0.5		0.246
	AP firing threshold	0.5 ± 0.5		0.246
	AP adaptation ratio	0.125 ± 0.125*	Σ=1	0.016
Dendritic morphology	Length per primary dendrite	0.5 ± 0.5		0.47
	Total dendritic length	0.5 ± 0.5		0.47
	Number of primary dendrites	0.125 ± 0.125*		0.03
	Dendritic polarity	0.125 ± 0.125*	Σ=1	0.03

Parameter weights were varied for each iteration of the CA using uniform distributions centered around 0.75, 0.5, and 0.25, respectively, with variations 0.125–0.5 ("average weight" and "weight variation"). Weights for each parameter group were normalized, such that axonal, electrical, and dendritic parameter sets had equal total weight. The average effective weights are also given (rightmost column). Asterisks indicate that parameters had weights >0 in only 25% of the iterations. This was implemented as weights randomly drawn from a uniform distribution centered around −0.25 with width 0.5 and a positivity cutoff for the weights. For the effect of altered weights on clustering results, compare Figure 10.

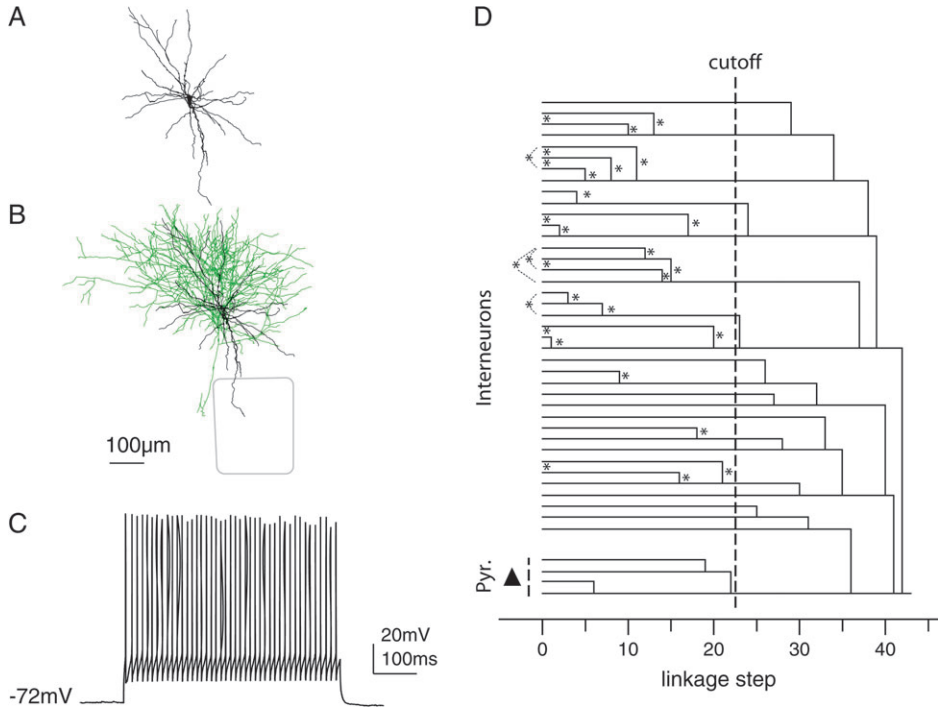

Figure 1. Illustration of parameter sets used in the feature vector for the CA. (*A*) The feature vector contained 4 parameters related to dendritic geometry: total dendritic length, length per primary dendrite, number of primary dendrites, and dendritic polarity index. (*B*) The feature vector contained 2 parameters related to axonal projection: laterality of axonal projection and verticality of axonal projection. (*C*) The feature vector contained 5 parameters related to electrical excitability: AP frequency adaptation ratio, AHP adaptation, AP half-width, input resistance at the soma, and AP threshold (for details, see text). (*D*) Linkage dendrogram for one CA iteration. The data matrix contained 39 INs and 4 L2/3 pyramidal neurons as control (black triangle). In each iteration, the weights of parameters were randomly varied (cf. Table 1), random variation was added to each data point, and a random number of neurons was excluded from the analysis. As cutoff (dashed line), the linkage step was chosen at which the pyramidal neurons were linked into one cluster. Then, all 2-neuron linkages that occurred up to that point were recorded (asterisks; in this CA 30 pairs of 2-neuron linkages were recorded).

OR). Single cluster analyses were cross-checked using STATISTICA for Windows (Statsoft, Tulsa, OK).

Stability of CAs

To analyze the stability of the iCA, 7 and 16 neurons were randomly excluded from the data matrix, and 1200 CAs were performed as described above, with maximal cluster sizes scaled to the smaller sample size (Supplementary Fig. 6). The stability to variation in overall parameter weights was investigated by reducing the sum weight of the dendritic, electrophysiological, and axonal parameters, respectively (Fig. 10 and Table 1; for details cf. Results).

Results

Iterated CA

We made CAs to define groups of INs. The CAs used 11 parameters. Four were related to dendritic geometry (Fig. 1*A*, cf. Helmstaedter et al. 2008b): 1) total dendritic length, 2) average length of primary dendrites, 3) number of primary dendrites, and 4) dendritic polarity. Two were related to axonal geometry (Fig. 1*B*, cf. Helmstaedter et al. 2008a): 5) laterality of axonal projections and 6) verticality of axonal projections. Five parameters were related to membrane excitability (Fig. 1*C*, cf. Helmstaedter et al. 2008b): 7) AP adaptation ratio, 8) AP-afterhyperpolarization (AHP) adaptation ratio, 9) AP half-width, 10) somatic input resistance, and 11) AP threshold.

The CA was repeated 1200 times. For each repetition, the weights for the 11 parameters were randomly varied within defined limits. These limits were chosen such that the dendritic, axonal, and electrical excitability parameters had equal total weights and that parameters which were shown to be correlated were assigned lower weights to reduce redundancy (cf. Table 1; the effects of altering the relative weights of dendritic, axonal, or electrical parameters are reported below, Fig. 10). In addition, all single data points were randomly varied within the error limits. Four L2/3 pyramidal cells were included into all CAs as positive control (for details cf. Methods).

Figure 1*D* shows the linkage plot for one particular CA out of 1200. The 4 pyramidal cells (triangle) are clustered at the 22nd linkage step (dashed line in Fig. 1*D*). This linkage step was used as cutoff such that all pairwise linkages between INs that occurred at smaller linkage distances were counted. The CA shown in Figure 1*D* yielded 30 pairwise associations between INs (asterisks in Fig. 1*D*). Note that for the derivation of average clusters, only pairs of associations were counted in the single CAs.

Figure 2*A* shows the histogram of pairwise associations that were detected in 1200 CAs. The *x*-axis represents all combinations of 2 cells drawn from the total of 43 cells in the analysis (39 INs, 4 control pyramidal neurons, i.e., 903 pairwise associations). Figure 2*B* shows the histogram from control runs with randomly assigned parameters. The level of associations in the control runs was interpreted as unspecific associations. Groups of INs were merged taking only the most frequent linkages that outreached 3 SDs of the normalized "noise histogram" (>200 observations, dashed line in Fig. 2*A*,*B*). Group sizes were set to a maximum of 5 INs (translaminar inhibitors), 6 INs (lateral inhibitors), and 7 INs (local inhibitors). Figure 2*A* shows that the 4 pyramidal neurons (indicated by a black triangles in Fig. 2*A*) were only linked in 85% of the analyses. This served as a negative control that the

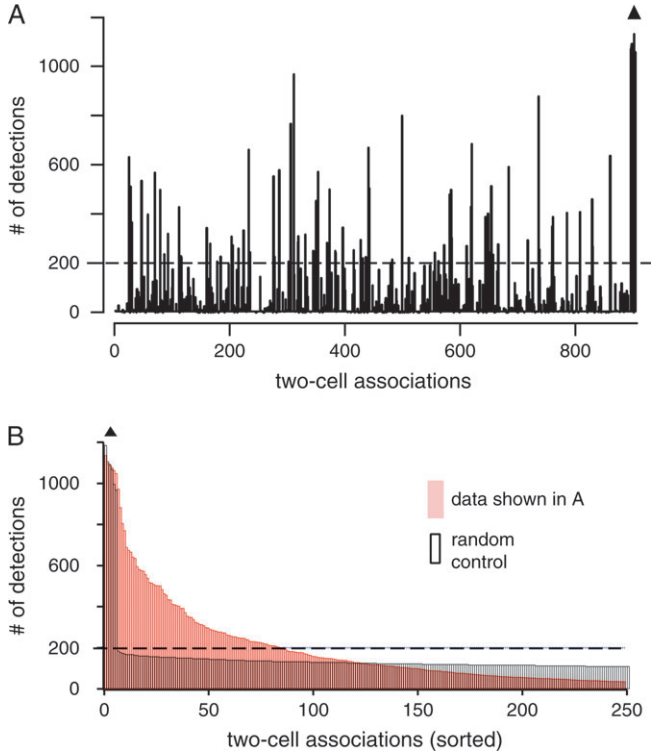

Figure 2. Associations after 1200 CAs. (*A*) Histogram of 2-neuron linkages that occurred in 1200 CAs of the type shown in Figure 1*D*. The number of pair associations is plotted against all 946 possible 2-neuron associations in a sample of 43 neurons. The 4 control pyramidal neurons clustered in >80% of the iterations (black triangle indicates the 6 pairwise pyramidal cell associations). (*B*) Histogram of control iterations. The data matrix was randomly shuffled for each parameter, such that only random associations should be detected. The histogram was sorted by detection count. Random control is shown in black, the original data (as in *A*) in red. Note that more than 70 associations were above threshold, whereas the majority was not (dashed lines in *A*, *B*). Only associations above threshold were used to link groups of INs (single linkage, starting with the most frequent associations).

added noise levels were large enough to distort existing group associations.

This approach is referred to as iCA. This iCA defined 9 groups of INs. Reconstructions of individual neurons belonging to 1 of the 9 groups of INs defined by the iCA are shown in Figures 6–10 and Supplementary Figures 1–4. Figure 11 displays the scheme of "axonal projection types" and IN groups as defined in this and the previous report (Helmstaedter et al. 2008a). The distributions of IN groups in the parameter space are shown by color code in Figures 3 and 4. For quantifications, cf. Tables 2–4 and Supplementary Tables 1–3.

Group Description

The following description of IN groups was a posteriori. It has to be emphasized that this description did not serve as the basis of classifications, but identified properties of the groups that were originally differentiated by the iCA. Groups *translaminar 1*, *lateral 1*, *local 1*, *local 2*, and *local 3* comprised ⩾4 neurons and are described in detail (Figs 5–9). Groups *translaminar 2*, *lateral 2*, *lateral 3*, and *local 4* comprised only 2 or 3 neurons and are treated in the Supplementary Figures 1–4.

Figure 5 shows group *translaminar 1* INs. This group comprised cells that had a dual axonal projection domain. One domain was located in L2/3 of the home column, and a second domain was located in lower layers 4 and 5A (Fig. 5). The

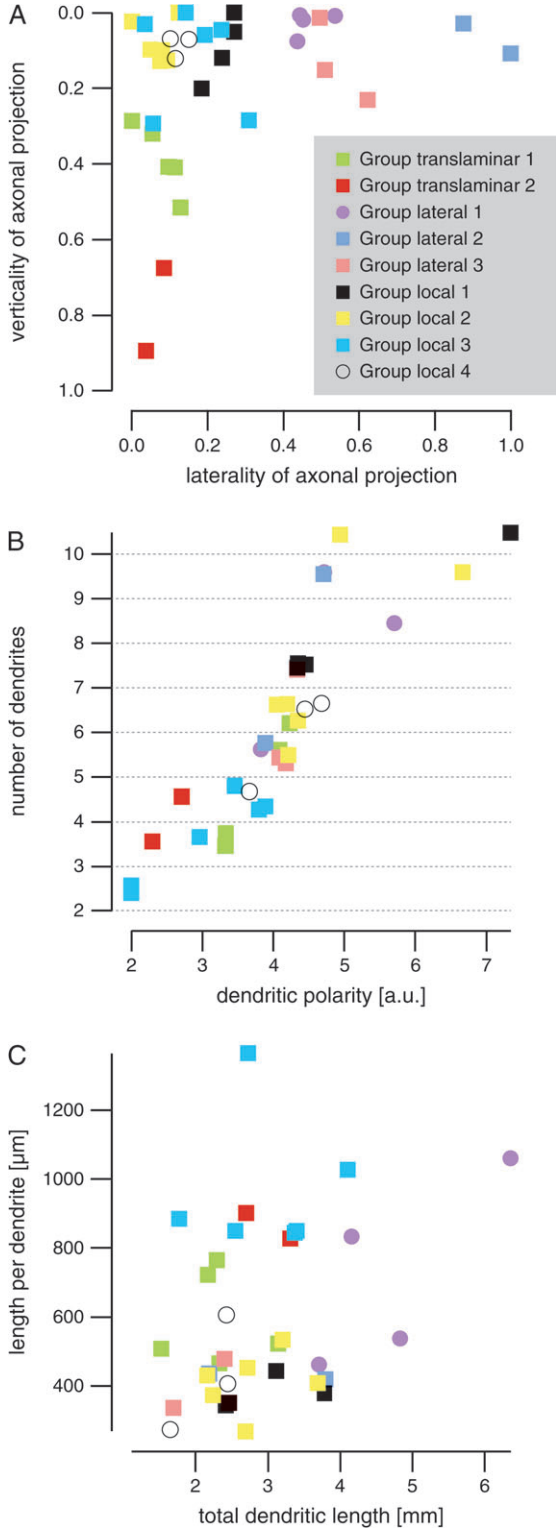

Figure 3. Distribution of groups of INs in the parameter space. (*A*) Distribution of groups of INs with respect to the 2 axonal parameters. Nine groups are shown in color code. (*B*, *C*) Distribution with respect to the 4 dendritic geometry parameters. For display in principal components space, compare Supplementary Figure 5. For quantifications, compare Tables 2 and 3.

dendritic arbors had a polarity index of 3.7 ± 0.4. This group of cells had a small AHP adaptation (0.63 ± 1.1 mV) and comparatively broad APs (0.5 ± 0.13 ms).

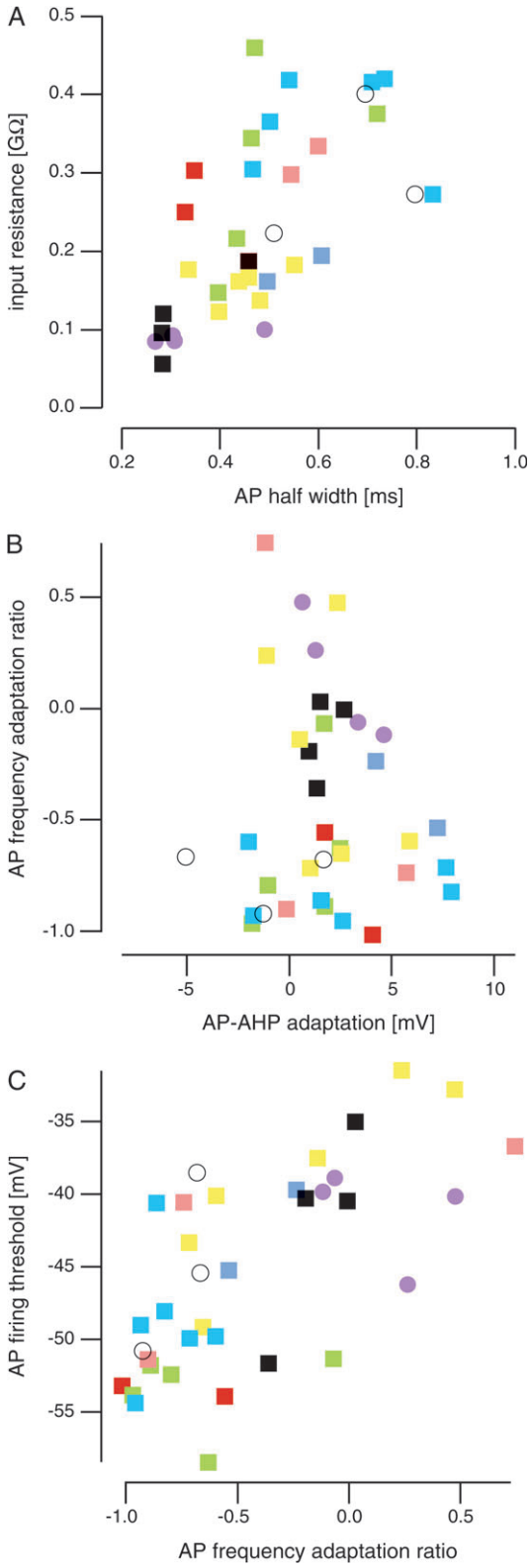

Figure 4. Distribution of groups of INs in the electrical excitability parameter space. Color code as in Figure 3. For quantifications, compare Table 4.

Figure 6 shows group *lateral 1* INs. They projected mainly to layer 2 of the home and the neighboring column (Fig. 6). Layer 1 was spared by the axonal arbor of these cells (note horizontal delineation of axonal projection at the L2–L1 border in Fig. 6). This group of cells had the largest dendritic trees of the sample (4.8 ± 1.15 mm total dendritic length, cf. Fig. 3*C* and Table 1). All cells had low somatic input resistance (91 ± 0.06 MΩ), small AP half-widths, and either none or positive AP frequency adaptation ratios (0.14 ± 0.28, Fig 4*C*) with a high AP threshold (–41 ± 3 mV, Fig. 4*C*).

Figure 7 shows group *local 1* INs with relatively dense axonal projections (30 ± 6 mm total axonal length) that had a smaller nonlocal contribution (11 ± 5% of the axon leaves the home column). Three of the 4 cells in this group projected mainly to layer 3. Group local 1 INs had the highest number of primary dendrites (7.7 ± 1.5). They were homogeneous in their passive and active membrane properties (Fig. 4, black squares). Group local 1 cells had very small AP half-widths and low somatic input resistances (0.33 ± 0.09 ms, 110 ± 52 MΩ, respectively) as well as little AP frequency and moderate AHP adaptation (–0.13 ± 0.18 and 1.6 ± 0.72 mV, respectively).

Group *local 2* (Fig. 8) comprised 6 cells with highly local axonal projections at a high density (total axonal length of 21 ± 5.6 mm). The cells had small dendritic trees with many short dendrites (2.8 ± 0.6 mm total dendritic length, 7 ± 2 dendrites with 410 ± 80 μm average length per dendrite, Figs. 3*B,C* and Table 2). They had a high AP firing threshold (–39 ± 6 mV), comparably low somatic input resistances (160 ± 20MΩ), and either no or positive AHP adaptation (1.9 ± 2.4 mV).

Group *local 3* cells are shown in Figure 9. The grouping of these cells was mainly caused by their similarity in dendritic and electrical excitability parameters. The axon of these cells was largely confined to the home column (94 ± 5% axon length within home column borders). The dendrites of group local 3 cells all entered layer 1. The cells had very broad APs (half-width 0.63 ± 0.15 ms), high somatic input resistance (370 ± 60 MΩ), and strongest AP frequency adaptation ratio with a low AP threshold (–0.82 ± 0.13, –49 ± 4 mV).

Relevance of Parameter Weights

We assessed the relevance of the dendritic, axonal, and electrical excitability parameters for the group assignments, respectively (Fig. 10). In the initial iCA described above, the relative parameter weights w_{dend}, w_{axon}, w_{ephys} were all equal. Here, we varied the relative parameter weights w_{dend}, w_{axon}, w_{ephys} systematically, and for each set of relative parameter weights $\{w_{dend}, w_{axon}, w_{ephys}\}$, an iCA was performed (1200 CAs each). Figure 10*A* shows that decreasing the axon parameter weights w_{axon} resulted in a strong declustering (color codes in Fig. 10 indicate group assignment of single INs). The reduction of dendrite parameter weights w_{dend} or the reduction of electrical excitability parameter weights w_{ephys} maintained largely stable group assignments (Figs 10*B,C*). A strong reduction of electrical excitability parameter weights w_{ephys}, however, reduced the difference between pyramidal cells and INs, such that for $w_{ephys} < 0.5$ most INs could not be assigned to groups unless pyramidal cells were misclassified as INs (Fig. 10*C*, for details of the iCA algorithm, cf. Methods).

Discussion

Significance of IN Group Definitions

Hierarchical CA was used before to define classes of INs quantitatively (e.g., Cauli et al. 2000; Krimer et al. 2005; Dumitriu et al. 2007). For a hierarchical CA, the choice of

Table 2

Average axonal parameters for groups, types (Helmstaedter et al. 2008a), and the whole sample of INs

	Verticality ratio	Laterality (a.u.)	Ratio of laterality	Lateral extent of axon (columns)	Total axonal length (mm)
Groups					
Translaminar 1 (n = 5)	0.39 ± 23%	0.079 ± 65%	0.016 ± 137%	0.27 ± 62%	8.4 ± 48%
Translaminar 2 (n = 2)	0.78 ± 19%	0.061 ± 54%	0.027 ± 26%	0.18 ± 86%	17 ± 45%
Lateral 1 (n = 4)	0.027 ± 118%	0.47 ± 9%	0.25 ± 38%	1.2 ± 12%	34 ± 29%
Lateral 2 (n = 2)	0.068 ± 81%	0.94 ± 9%	0.49 ± 12%	2.5 ± 10%	29 ± 32%
Lateral 3 (n = 3)	0.13 ± 83%	0.54 ± 12%	0.22 ± 33%	1.6 ± 17%	19 ± 48%
Local 1 (n = 4)	0.092 ± 93%	0.24 ± 16%	0.11 ± 45%	0.66 ± 22%	30 ± 19%
Local 2 (n = 6)	0.079 ± 68%	0.071 ± 60%	0.025 ± 125%	0.22 ± 52%	21 ± 27%
Local 3 (n = 6)	0.12 ± 112%	0.16 ± 65%	0.064 ± 84%	0.49 ± 62%	9.5 ± 64%
Local 4 (n = 3)	0.087 ± 34%	0.12 ± 20%	0.055 ± 37%	0.36 ± 19%	9.5 ± 44%
Chandelier (n = 2)	0.041 ± 130%	0.033 ± 1%	0.005 ± 73%	0.12 ± 8%	37 ± 18%
Types					
Local inhibitors (n = 20)	0.063 ± 89%	0.15 ± 58%	0.073 ± 98%	0.42 ± 53%	18 ± 54%
Lateral inhibitors (n = 15)	0.1 ± 91%	0.056 ± 36%	0.28 ± 44%	1.5 ± 40%	24 ± 46%
Translaminar inhibitors (n = 10)	0.51 ± 39%	0.066 ± 59%	0.015 ± 122%	0.33 ± 60%	14 ± 80%
L1 inhibitors (n = 4)	0.0096 ± 147%	0.38 ± 51%	0.21 ± 64%	0.92 ± 50%	23 ± 36%
All groups and ungrouped (n = 51)	0.16 ± 130%	0.27 ± 90%	0.13 ± 106%	0.73 ± 90%	20 ± 55%

Values are mean ± SD given in percent of the mean for comparison of parameters. For distribution plots of the axonal parameters, compare Figure 3; reconstructions of axonal arbors are shown in Figures 5–9 and Supplementary Figures 1–4.

Table 3

Average dendritic parameters for groups, types (Helmstaedter et al. 2008a), and the whole sample of INs

	Dendritic polarity (a.u.)	Number of primary dendrites	Length per primary dendrite (μm)	Total dendritic length (mm)
Groups				
Translaminar 1 (n = 5)	3.7 ± 12%	4 ±35%	600 ± 22%	2.3 ± 25%
Translaminar 2 (n = 2)	2.5 ± 11%	3.5 ± 20%	860 ± 5%	3 ± 14%
Lateral 1 (n = 4)	4.6 ± 18%	7 ± 26%	720 ± 38%	4.8 ± 24%
Lateral 2 (n = 2)	4.3 ± 13%	7 ± 40%	430 ± 2%	3 ± 37%
Lateral 3 (n = 3)	4.2 ± 3%	5.7 ± 20%	390 ± 20%	2.2 ± 19%
Local 1 (n = 4)	5.1 ± 28%	7.7 ± 19%	380 ± 11%	2.9 ± 21%
Local 2 (n = 6)	4.7 ± 21%	7 ± 28%	410 ± 21%	2.8 ± 20%
Local 3 (n = 6)	3 ± 28%	3.2 ± 31%	970 ± 21%	3 ± 27%
Local 4 (n = 3)	4.3 ± 12%	5.3 ± 21%	430 ± 38%	2.2 ± 20%
Chandelier (n = 1)	3.3	3	910	2.7
Types				
Local inhibitors (n = 19)	4.4 ± 28%	6.1 ± 41%	550 ± 52%	2.8 ± 21%
Lateral inhibitors (n = 14)	4 ± 21%	5.7 ± 35%	670 ± 50%	3.5 ± 38%
Translaminar inhibitors (n = 10)	3.4 ± 23%	4 ± 31%	700 ± 29%	2.7 ± 26%
L1 inhibitors (n = 4)	3.6 ± 18%	4.2 ± 35%	860 ± 52%	3.2 ± 29%
All groups and ungrouped (n = 56)	3.9 ± 27%	5.1 ± 42%	660 ± 48%	2.9 ± 33%

Values are mean ± SD given in percent of the mean for comparison of parameters. For distribution plots of the dendritic parameters, compare Figure 3; reconstructions of dendrites are shown in Figures 5–9 and Supplementary Figures 1–4.

Table 4

Average electrical excitability parameters for groups, types (Helmstaedter et al. 2008a), and the whole sample of INs

	Input resistance (MΩ)	AP half-width (ms)	AP frequency adaptation ratio	AHP adaptation (mV)	AP threshold potential (mV)
Groups					
Translaminar 1 (n = 5)	310 ± 40%	0.5 ± 25%	−0.67 ± 53%	0.63 ± 304%	−54 ± 5%
Translaminar 2 (n = 2)	280 ± 13%	0.34 ± 3%	−0.79 ± 41%	2.9 ± 56%	−54 (n=1)
Lateral 1 (n = 4)	91 ± 7%	0.34 ± 29%	0.14 ± 199%	2.5 ± 74%	−41 ± 8%
Lateral 2 (n = 2)	180 ± 13%	0.55 ± 14%	−0.39 ± 55%	5.7 ± 37%	−42 ± 9%
Lateral 3 (n = 3)	270 ± 27%	0.53 ±13%	−0.3 ± 304%	1.5 ± 250%	−43 ± 17%
Local 1 (n = 4)	110 ± 47%	0.33 ± 26%	−0.13 ± 137%	1.6 ± 45%	−42 ± 16%
Local 2 (n = 6)	160 ± 14%	0.44 ± 16%	−0.23 ± 218%	1.9 ± 126%	−39 ± 16%
Local 3 (n = 6)	370 ± 17%	0.63 ± 23%	−0.82 ± 16%	2.7 ± 162%	−49 ± 9%
Local 4 (n = 3)	300 ± 30%	0.67 ± 21%	−0.76 ± 19%	−1.5 ± 217%	−45 ± 13%
Chandelier (n = 2)	130 ± 22%	0.23 ± 3%	0.053 ± 408%	1.1 ± 69%	−41 ± 16%
Types					
Local inhibitors (n = 19)	240 ± 59%	0.51 ± 32%	−0.48 ± 89%	0.98 ± 350%	−44 ± 16%
Lateral inhibitors (n = 15)	220 ± 56%	0.55 ± 38%	−0.33 ± 158%	2.4 ± 149%	−45 ± 16% (n = 13)
Translaminar inhibitors (n = 10)	290 ± 39%	0.48 ± 27%	−0.63 ± 63%	1.6 ± 180%	−52 ± 7% (n = 9)
L1 inhibitors (n = 4)	200 ± 24%	0.76 ± 52%	−0.64 ± 18%	7.9 ± 46%	−46 ± 21% (n = 2)
All groups and ungrouped (n = 64)	260 ± 53%	0.54 ± 41%	−0.5 ± 86%	2.1 ± 171%	−46 ± 17% (n = 56)

Values are mean ± SD given in percent of the mean for comparison of parameters. For distribution plots of the electrical excitability parameters, compare Figure 4.

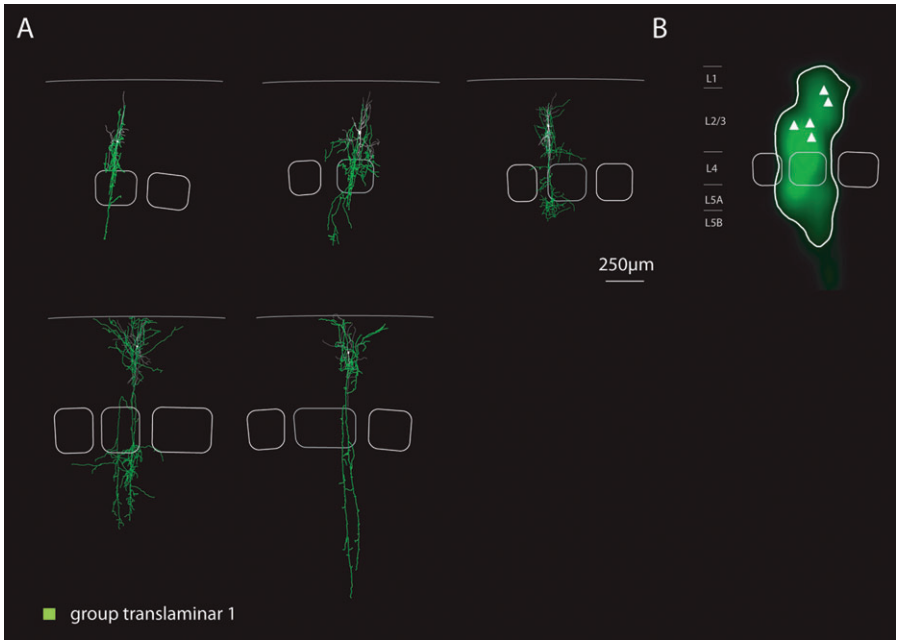

Figure 5. Group *translaminar 1* INs. (*A*) Reconstructions and (*B*) average axonal density map. This group comprised cells with a dual axonal projection domain. One domain was located in L2/3 of the home column, and a second domain was located in lower layers 4 and 5A. The dendritic arbors had a polarity index of 3.7 ± 0.4. This group of cells had a small AHP adaptation (0.63 ± 1.1 mV) and broad APs (0.5 ± 0.13 ms).

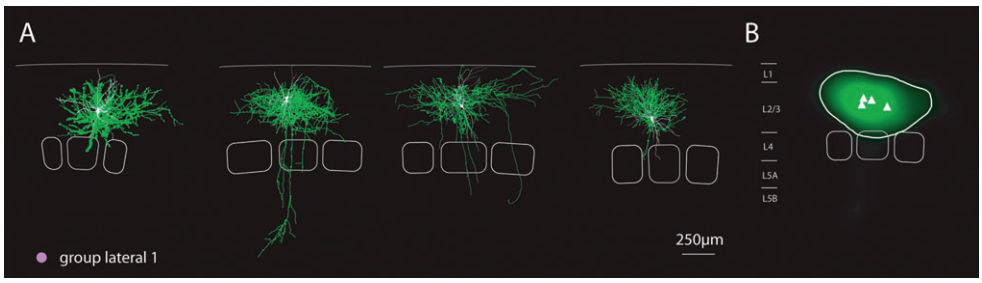

Figure 6. Group *lateral 1* INs. (*A*) Reconstructions and (*B*) average axonal density map. Group lateral 1 INs projected mainly to layer 2 of the home and the neighboring column. Layer 1 was spared by the axonal arbor of these cells (note horizontal delineation of axonal projection at the L2–L1 border). This group of cells had the largest dendritic trees of the sample (4.8 ± 1.15 mm total dendritic length, cf. Fig. 3*C* and Table 3). All cells had low somatic input resistance (91 ± 0.06 MΩ), small AP half-widths, and either none or positive AP frequency adaptation ratios (0.14 ± 0.28, Fig. 4*C*) with a high AP threshold (−41 ± 3 mV, Fig. 4*C*).

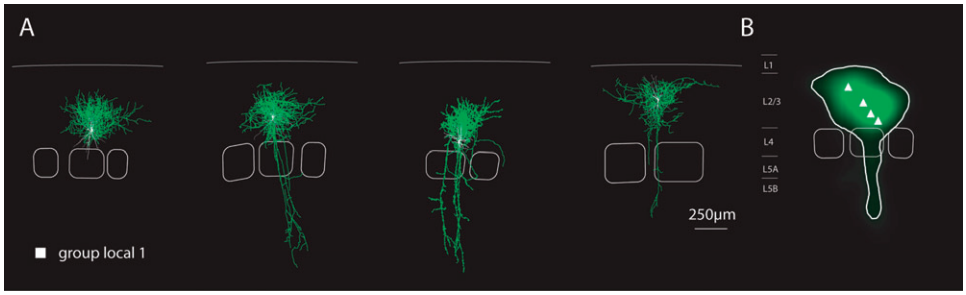

Figure 7. Group *local 1* INs. (*A*) Reconstructions and (*B*) average axonal density map. Group local 1 INs had very dense axonal projections (30 ± 6 mm total axonal length) that had a minor nonlocal contribution (11 ± 5% of the axon left the home column). Three of the 4 cells in this group projected mainly to L3. Group local 1 cells had the highest number of primary dendrites (7.7 ± 1.5). They were homogeneous in their passive and active membrane properties (Fig. 4, black squares). They had very small AP half-widths and low somatic input resistances (0.33 ± 0.09 ms, 110 ± 52 MΩ, respectively) as well as little AP frequency and AHP adaptation (−0.13 ± 0.18 and 1.6 ± 0.72 mV, respectively).

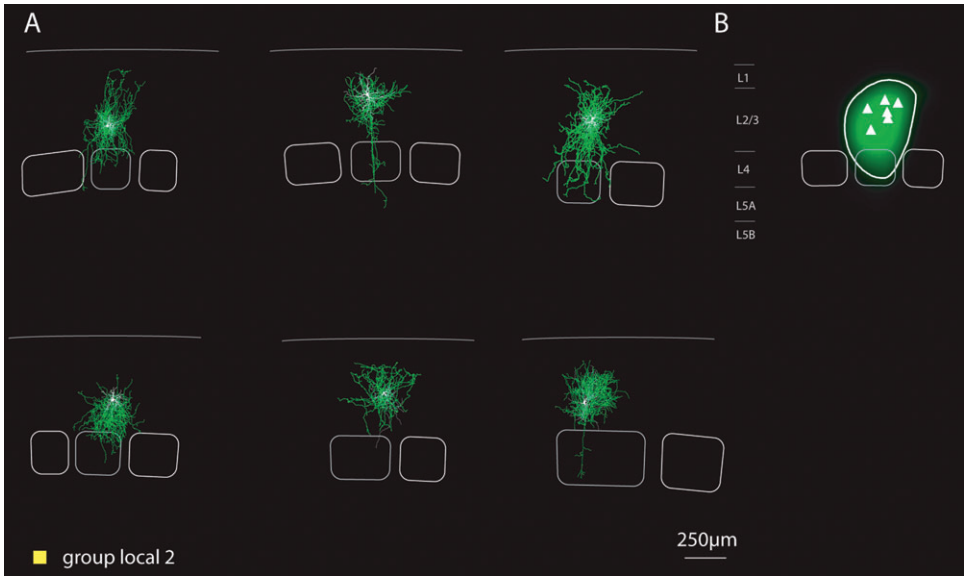

Figure 8. Group *local 2* INs. (*A*) Reconstructions and (*B*) average axonal density map. Group local 2 comprised 6 cells with highly local axonal projections at a high density (total axonal length of 21 ± 5.6 mm). The cells had short dendritic trees with many short dendrites (2.8 ± 0.6 mm total dendritic length, 7 ± 2 dendrites with 410 ± 80 µm average length per dendrite, Figs 3*B*,*C* and Table 3). They had a high AP firing threshold (−39 ± 6 mV), comparably low somatic input resistances (160 ± 20 MΩ), and either none or positive AHP adaptation (1.9 ± 2.4 mV).

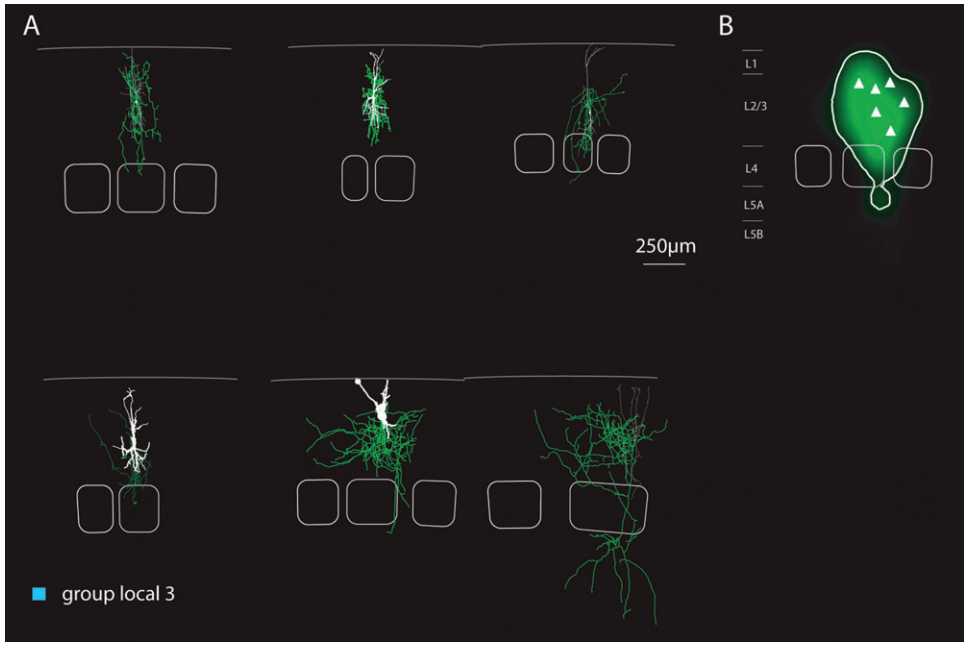

Figure 9. Group *local 3*-INs. (*A*) Reconstructions and (*B*) average axonal density map. The grouping of these cells was mainly caused by their similarity in electrical excitability and dendritic parameters. The axon of these cells was largely confined to the home column (94 ± 5% axon length within home column borders). The dendrites of group local 3 cells all entered L1. These neurons had very broad APs (half-width 0.63 ± 0.15 ms), high somatic input resistance (370 ± 60 MΩ), and strongest AP frequency adaptation ratio with a low AP threshold (−0.82 ± 0.13, −49 ± 4 mV. respectively).

parameter sets and the choice of weights for each parameter set are crucial. Because the validity of weights and the relevance of parameter sets are typically not known a priori, we added iterations to the CA that allowed to randomly vary the weights of parameter sets as well as the data points within the parameter sets ("iterated" CA).

The iCA presented here was thus aimed at using only the most significant clusterings for the definition of IN groups. Significance of clustering was defined as above-chance similarity in repeated CAs using noisy parameter sets. Thus, the 3 main features of the iCA were 1) addition of noise to all parameters and sampling of the most frequent clusterings, 2) addition

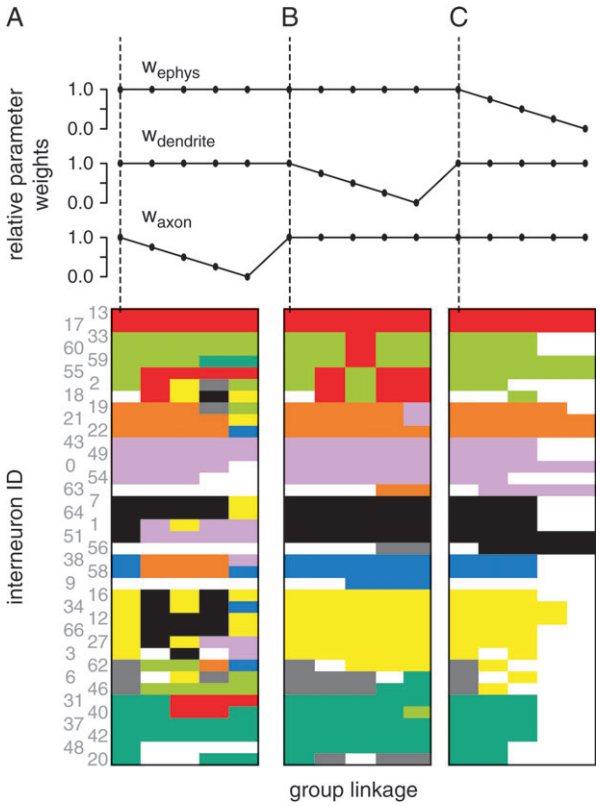

Figure 10. Stability of group detection to varying weights of parameter sets. A total of 13 iCAs (1200 CA each) were made with varying relative weights of the electrical, dendritical, and axonal parameter sets w_{ephys}, w_{dend}, w_{axon}. The first column shown is the unaltered iCA ($w_{ephys} = w_{dend} = w_{axon}$; dashed vertical lines). (*A*) Group detection is shown for decreasing relative axonal parameter weight w_{axon}; (*B*) for decreasing relative dendritic parameter weight w_{dend}; (*C*) for decreasing relative electrical parameter weight w_{ephys}. Reduction of the axonal parameter weight w_{axon} resulted in declustering (*A*), whereas the other 2 parameter groups maintained relatively stable group assignments (*B*, *C*). Note that for reduction of the electrical parameter weight $w_{ephys} < 0.5$, most INs could not be assigned to groups unless pyramidal neurons were misclassified as INs (see Results). For details on the chosen parameter weights, compare Methods and Table 1.

of a pyramidal cell group as control for intracluster distance, and 3) impairment of large cluster sizes using a cluster size penalty.

The addition of further neurons to the analysis should therefore only yield new groups if the added neurons were significantly close in the parameter space (see Supplementary Fig. 6). In the present data set, 10% (4 of 39) INs were not assigned to groups by the iCA. In our sample, 5 of 9 groups comprised ⩾4 neurons. Although even 2-neuron linkages were significant, for intergroup comparisons, a larger group size was required. We therefore present the 5 groups with ⩾ 4 neurons as the main result of this study as is illustrated in the scheme of Figure 11.

Currently available data on morphological properties of neurons is typically limited to small (<100 cells) data sets. The precision and significance of clustering is expected to increase with the availability of very large morphological data sets as can possibly be obtained using large-volume serial-sectioning electron microscopy techniques (for a review, see Briggman and Denk 2006).

IN group definitions could be independently validated by investigating properties of the groups that were not used for clustering. In a subsequent study, we therefore investigated the properties of synaptic input from L4 spiny neurons to the IN groups presented here (Helmstaedter et al. 2008c).

Previous Descriptions of IN Classes

Since the early work of Ramón y Cajal (1904), numerous "classes" of INs have been described qualitatively (Lorente de No 1938; Jones 1975; Gupta et al. 2000). The distinction between within-class variance and across-class variance was assessed on qualitative grounds, mainly by visual inspection. Even electrical excitability was evaluated qualitatively (Gupta et al. 2000). The present study was designed to make use of quantified parameters without qualitative preselection. Therefore, it was possible to relate the emerging groups a posteriori to previously described classifications (see Supplementary Table 3 for an overview).

"Basket" cells were described first by Ramón y Cajal (1904) in the cerebellum. The name-giving property was considered to be the formation of axonal perisomatic baskets formed around postsynaptic cells. Early studies using staining of multiple cells suggested extensive plexus formed by single basket cells (Marin-Padilla 1969). The first quantitative studies (Somogyi et al. 1983; Somogyi and Soltesz 1986), however, revealed that the presumed basket cells projected only about 20–30% of their boutons to pyramidal cell somata for forming the baskets, meaning that 70–80% of the boutons do not target somata (Ramón y Cajal 1904; Marin-Padilla 1969; Szentagothai 1973; Di Cristo et al. 2004). A single basket cell only contributed a few branches each to perisomatic arborizations. In addition, other INs contribute to the pericellular baskets (White and Keller 1989). Other properties have been ascribed to basket cells. Their dendrites were designated as multipolar, and the AP pattern was described as fast spiking. Two groups of neurons in the present analysis could match this description: group lateral 1 and group local 1 (Figs 6 and 7). Their main distinction was the axonal projection type, separating lateral inhibitors from local inhibitors. The group lateral 2 cells (s. Supplementary material, Figure 2) might also be considered basket cells by some authors (Wang et al. 2002).

Neurogliaform cells date also back to descriptions by Ramón y Cajal (1904) who used the terms spider web or dwarf cells. Neurogliaform cells were referred to by some authors (Jones 1984; Ferrer and Sancho 1987; Kisvarday et al. 1990; Hestrin and Armstrong 1996; Tamas et al. 2003; Simon et al. 2005; Povysheva et al. 2007) and described neurons with very small dendritic and axonal trees. Group local 2 cells could match this description (Fig. 8).

Bitufted neurons were also first described by Ramón y Cajal. As pointed out (Ramón y Cajal 1904; Somogyi and Cowey 1984), their name-giving property, the tufted bipolar dendritic tree, is not as distinctive as their narrow axonal projection. This discrepancy between name and separation properties has led to several different nomenclatures for INs with a small number of dendrites. In addition, bipolar neurons were described (Feldman and Peters 1978). The present grouping did not support the segregation into bipolar and bitufted cells. As shown (Helmstaedter et al. 2008b), the polarity of the dendritic arbor was not predictive for the axon projection. Groups translaminar 1, translaminar 2, local 3, and local 4 (Figures 5, 9, Supplementary Figures 1,4) contained cells with bipolar or bitufted dendritic morphologies. These groups comprised either local or translaminar inhibitors with axonal trees restricted to the home column.

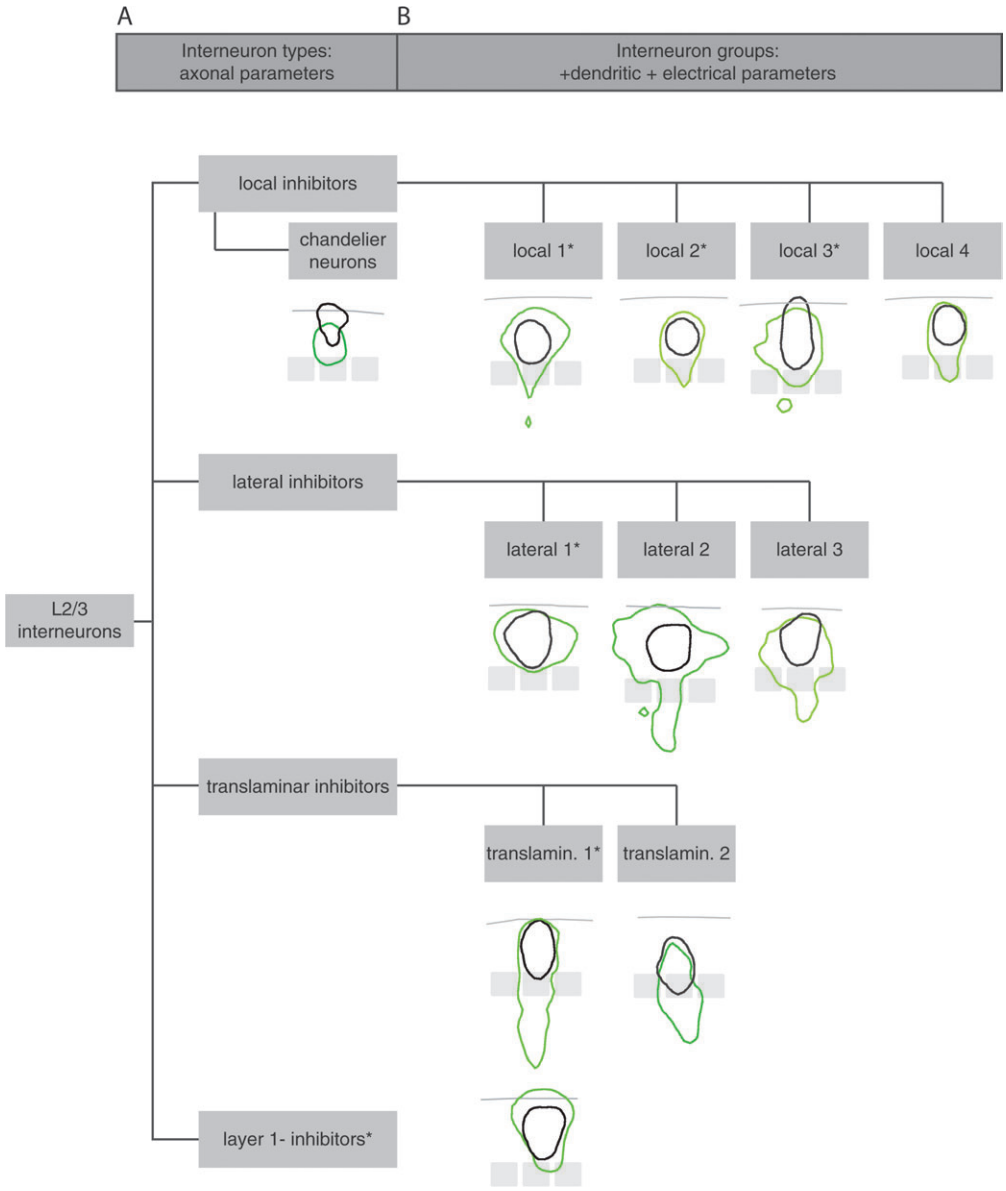

Figure 11. Scheme of IN types and groups. (*A*) A quantitative analysis of axonal projections yielded the definition of 4 main types of INs that established common innervation domains with reference to cortical columns: local, lateral, translaminar, and L1 inhibitors (Helmstaedter et al. 2008a). "Chandelier neurons" also showed local axonal projections. Local, lateral, and translaminar inhibitors comprised INs with heterogeneous dendritic and electrical parameters. These were therefore further analyzed using the iCAs presented in this study. (*B*) The multiparameter analysis including axonal, dendritic, and electrical parameters identified 9 groups of INs that had common innervation domains (defined by their type of axonal projection, Helmstaedter et al. 2008a) and in addition had common dendritic geometry and electrical excitability parameters. Insets: average outlines of axonal (green) and dendritic (black) domains are shown as 90% contour lines for each group, superimposed on an average barrel pattern. Asterisks indicates selection of groups with $\geq$4 neurons in the sample (cf. Figs 5–9). For groups with $<$4 neurons in the sample, reconstructions are shown in Supplementary Figures 1–4.

Low-threshold spiking (LTS) cells were classified based on their intrinsic electrical excitability (Connors and Gutnick 1990; Kawaguchi and Kubota 1993; Gibson et al. 1999). These neurons generated low-threshold depolarizations in response to current stimuli that gave rise to bursts of APs. Figure 4*C* shows that group translaminar 1, translaminar 2, and group local 3 cells matched this criterion. The LTS criterion was however also fulfilled for some neurons in other groups. Electrical excitability measures alone were a poor predictor of axonal projection types (Helmstaedter et al. 2008b).

Two recent studies suggested a classification of INs based on immunohistochemical marker expression at different stages of postnatal development (Miyoshi et al. 2007; Gonchar et al. 2008), proposing 7 and 13 groups of INs, respectively. This number is in the range of IN groups reported in this study (9 + chandelier neurons and L1 inhibitors = 11 groups, cf. Fig. 11).

Applicability to Pyramidal Neurons

The analysis of axonal projection patterns as the main distinctive property of neurons could be applied to the subclassification of pyramidal neurons as well. The axonal projection of pyramidal neurons is typically to subcortical areas, and the target areas of these neurons can be used as a criterion for classification (Hattox and Nelson 2007).

Cortical Areas

We made use of the column geometry as reference frame for the analysis of axon projection types. The primary somatosensory cortex of rodents is uniquely suited for this type of analysis because the column borders are easily delineable. In other primary sensory areas, ensembles of neurons with common receptive properties are less clearly separated anatomically. It will require detailed reconstructions of large areas of neocortical tissue (e.g., Briggman and Denk 2006) to clarify whether within the more complex module structure of, for example, visual cortices, the INs show analogous types of axonal projection with reference to the representational borders.

Outlook

The presented definition of IN groups is an attempt to quantify the contribution of inhibition to the sensory representation in a cortical column. The next steps are to analyze the synaptic input and the synaptic output of the 4 types and 9 groups of INs (see Fig. 11) that are suggested here (Helmstaedter et al. 2008c). In addition, in vivo recordings from single cortical INs in L2/3 with reconstructions of dendritic and axonal geometry are necessary to analyze the receptive field structure and in vivo responsiveness of these neurons (Hirsch et al. 2003; Zhu et al. 2004). Together, this data may allow constructing mechanistic models of a cortical column that implement morphological and physiological constraints on excitatory and inhibitory processing of sensory stimuli (Helmstaedter et al. 2007; Douglas and Martin 2007).

Supplementary Material

Supplementary material can be found at: http://www.cercor.oxfordjournals.org/.

Funding

This work was supported by the Max-Planck Society.

Notes

The authors would like to thank Drs Arnd Roth and Andreas Schaefer for fruitful discussions and Drs Jochen Staiger and Andreas Schaefer for helpful comments on previous versions of the manuscript. *Conflict of Interest*: None declared.

Address correspondence to Moritz Helmstaedter, Department of Cell Physiology, Max-Planck Institute for Medical Research, Jahnstrasse 29, D-69120 Heidelberg, Germany. Email: moritz.helmstaedter@mpimf-heidelberg.mpg.de.

References

Agmon A, Connors BW. 1991. Thalamocortical responses of mouse somatosensory (barrel) cortex in vitro. Neuroscience. 41:365–379.

Beaulieu C. 1993. Numerical data on neocortical neurons in adult rat, with special reference to the GABA population. Brain Res. 609:284–292.

Briggman KL, Denk W. 2006. Towards neural circuit reconstruction with volume electron microscopy techniques. Curr Opin Neurobiol. 16:562–570.

Cauli B, Porter JT, Tsuzuki K, Lambolez B, Rossier J, Quenet B, Audinat E. 2000. Classification of fusiform neocortical interneurons based on unsupervised clustering. Proc Natl Acad Sci USA. 97:6144–6149.

Connors BW, Gutnick MJ. 1990. Intrinsic firing patterns of diverse neocortical neurons. Trends Neurosci. 13:99–104.

Di Cristo G, Wu C, Chattopadhyaya B, Ango F, Knott G, Welker E, Svoboda K, Huang ZJ. 2004. Subcellular domain-restricted GABAergic innervation in primary visual cortex in the absence of sensory and thalamic inputs. Nat Neurosci. 7:1184–1186.

Dodt HU, Zieglgansberger W. 1990. Visualizing unstained neurons in living brain slices by infrared DIC-videomicroscopy. Brain Res. 537:333–336.

Douglas RJ, Martin KA. 2007. Mapping the matrix: the ways of neocortex. Neuron. 56:226–238.

Dumitriu D, Cossart R, Huang J, Yuste R. 2007. Correlation between axonal morphologies and synaptic input kinetics of interneurons from mouse visual cortex. Cereb Cortex. 17:81–91.

Feldman ML, Peters A. 1978. The forms of non-pyramidal neurons in the visual cortex of the rat. J Comp Neurol. 179:761–793.

Feldmeyer D, Egger V, Lübke J, Sakmann B. 1999. Reliable synaptic connections between pairs of excitatory layer 4 neurones within a single 'barrel' of developing rat somatosensory cortex. J Physiol. 521:169–190.

Ferrer I, Sancho S. 1987. Non-pyramidal neurons of layers I-III in the dog's cerebral cortex (parietal lobe). A Golgi survey. Acta Anat (Basel). 129:43–52.

Gibson JR, Beierlein M, Connors BW. 1999. Two networks of electrically coupled inhibitory neurons in neocortex. Nature. 402:75–79.

Gonchar Y, Wang Q, Burkhalter A. 2008. Multiple distinct subtypes of GABAergic neurons in mouse visual cortex identified by triple immunostaining. Front Neuroanat. 1:3. doi:10.3389/neuro.05/003.

Gupta A, Wang Y, Markram H. 2000. Organizing principles for a diversity of GABAergic interneurons and synapses in the neocortex. Science. 287:273–278.

Hattox AM, Nelson SB. 2007. Layer V neurons in mouse cortex projecting to different targets have distinct physiological properties. J Neurophysiol. 98:3330–3340.

Helmstaedter M, de Kock CP, Feldmeyer D, Bruno RM, Sakmann B. 2007. Reconstruction of an average cortical column in silico. Brain Res Rev. 55:193–203.

Helmstaedter M, Sakmann B, Feldmeyer D. 2008a. Neuronal correlates of lateral, local and translaminar inhibition with reference to cortical columns. Cerebral Cortex. doi:10.1093/cercor/bhn141.

Helmstaedter M, Sakmann B, Feldmeyer D. 2008b. The relation between dendritic geometry, electrical excitability, and axonal projections of L2/3 interneurons in rat barrel cortex. Cerebral Cortex. doi:10.1093/cercor/bhn138.

Helmstaedter M, Staiger JF, Sakmann B, Feldmeyer D. 2008c. Differential recruitment of layer 2/3 interneuron groups by layer 4 input in single columns of rat somatosensory cortex. J Neurosci. 28:8273–8284.

Hestrin S, Armstrong WE. 1996. Morphology and physiology of cortical neurons in layer I. J Neurosci. 16:5290–5300.

Hirsch JA, Martinez LM, Pillai C, Alonso J, Wang Q, Sommer FT. 2003. Functionally distinct inhibitory neurons at the first stage of visual cortical processing. Nat Neurosci. 6:1300–1308.

Jones EG. 1975. Varieties and distribution of non-pyramidal cells in the somatic sensory cortex of the squirrel monkey. J Comp Neurol. 160:205–267.

Jones EG. 1984. Neurogliaform or spiderweb cells. In: Peters A, Jones EG, editors. Cerebral cortex: cellular components of the cerebral cortex. New York: Plenum Press. p. 409–418.

Kawaguchi Y, Kubota Y. 1993. Correlation of physiological subgroupings of nonpyramidal cells with parvalbumin- and calbindinD28k-immunoreactive neurons in layer V of rat frontal cortex. J Neurophysiol. 70:387–396.

Kisvarday ZF, Gulyas A, Beroukas D, North JB, Chubb IW, Somogyi P. 1990. Synapses, axonal and dendritic patterns of GABA-immunoreactive neurons in human cerebral cortex. Brain. 113:793–812.

Krimer LS, Zaitsev AV, Czanner G, Kroner S, Gonzalez-Burgos G, Povysheva NV, Iyengar S, Barrionuevo G, Lewis DA. 2005. Cluster analysis-based physiological classification and morphological properties of inhibitory neurons in layers 2-3 of monkey dorsolateral prefrontal cortex. J Neurophysiol. 94:3009–3022.

Lorente de No R. 1938. Cerebral cortex: architecture, intracortical connections, motor projections (chapter 15). In: Fulton JF, editor. Physiology of the nervous system. Oxford: Oxford University Press. p. 288–313.

Lübke J, Roth A, Feldmeyer D, Sakmann B. 2003. Morphometric analysis of the columnar innervation domain of neurons connecting layer 4

and layer 2/3 of juvenile rat barrel cortex. Cereb Cortex. 13: 1051–1063.
Marin-Padilla M. 1969. Origin of the pericellular baskets of the pyramidal cells of the human motor cortex: a Golgi study. Brain Res. 14:633–646.
Miyoshi G, Butt SJ, Takebayashi H, Fishell G. 2007. Physiologically distinct temporal cohorts of cortical interneurons arise from telencephalic Olig2-expressing precursors. J Neurosci. 27:7786–7798.
Povysheva NV, Zaitsev AV, Kroner S, Krimer OA, Rotaru DC, Gonzalez-Burgos G, Lewis DA, Krimer LS. 2007. Electrophysiological differences between neurogliaform cells from monkey and rat prefrontal cortex. J Neurophysiol. 97:1030–1039.
Ramón y Cajal S. 1904. Textura del sistema nervioso del hombre y de los vertebrados. Madrid (Spain): Imprenta N. Moya.
Simon A, Olah S, Molnar G, Szabadics J, Tamas G. 2005. Gap-junctional coupling between neurogliaform cells and various interneuron types in the neocortex. J Neurosci. 25:6278–6285.
Somogyi P, Cowey A. 1984. Double bouquet cells. In: Peters A, Jones EG, editors. Cerebral cortex: cellular components of the cerebral cortex. New York: Plenum Press. p. 337–360.
Somogyi P, Kisvarday ZF, Martin KA, Whitteridge D. 1983. Synaptic connections of morphologically identified and physiologically characterized large basket cells in the striate cortex of cat. Neuroscience. 10:261–294.
Somogyi P, Soltesz I. 1986. Immunogold demonstration of GABA in synaptic terminals of intracellularly recorded, horseradish peroxidase-filled basket cells and clutch cells in the cat's visual cortex. Neuroscience. 19:1051–1065.
Stuart GJ, Dodt HU, Sakmann B. 1993. Patch-clamp recordings from the soma and dendrites of neurons in brain slices using infrared video microscopy. Pflugers Arch. 423:511–518.
Szentagothai J. 1973. Synaptology of the visual cortex. In: Jung R, editor. Handbook of sensory physiology. New York: Springer-Verlag, p. 269–324.
Tamas G, Lorincz A, Simon A, Szabadics J. 2003. Identified sources and targets of slow inhibition in the neocortex. Science. 299:1902–1905.
Wang Y, Gupta A, Toledo-Rodriguez M, Wu CZ, Markram H. 2002. Anatomical, physiological, molecular and circuit properties of nest basket cells in the developing somatosensory cortex. Cereb Cortex. 12:395–410.
White EL, Keller A. 1989. Cortical circuits: synaptic organization of the cerebral cortex: structure, function, and theory. Boston (MA): Birkhäuser.
Zhu Y, Stornetta RL, Zhu JJ. 2004. Chandelier cells control excessive cortical excitation: characteristics of whisker-evoked synaptic responses of layer 2/3 nonpyramidal and pyramidal neurons. J Neurosci. 24:5101–5108.